

# CW Atom Laser

## Final Progress Report

Georg Raithel

*FOCUS Center, Physics Department, University of Michigan  
450 Church St., Ann Arbor, MI 48109*

### I. PROBLEM UNDER INVESTIGATION

A continuous-wave (cw), phase- and amplitude-stable atom laser based on magnetic guiding, magnetic compression, and continuous distributed evaporative cooling has been pursued. The detailed work has included the fabrication of a long, high-gradient magnetic atom guide, the development of in-situ probing techniques for magnetically guided atomic beams, and the development of methods to continuously operate and evaporatively cool such beams. Progress has been made towards a flux increase that will be essential to achieve efficient evaporative atomic-beam cooling. In the future, a cw Bose-Einstein condensate (BEC) shall be formed near the end of a linear magnetic atom guide in a potential well embedded in the guide. A coherent cw matter-wave beam will be extracted from the BEC through a tunneling barrier. This source of coherent matter waves will be ideal for atom-interferometric field- and motion sensors, which may become the sensing and navigation instrumentation of the future.

### II. MOST IMPORTANT RESULTS

We have demonstrated the continuous injection and propagation of a cold atomic beam in a high-gradient (up to 2.7 kG/cm) magnetic guide of 1.7 m length. Continuous injection is accomplished using a side-loading scheme that involves a sequence of two modified magneto-optic traps. An open-channel imaging method has been developed that allowed us to measure the atomic-flow temperatures and the flux under steady-state conditions. In the present implementation of the guide, the atomic beam in the high-gradient portion of the guide has been found to have a transverse temperature of  $420 \mu\text{K} \pm 40 \mu\text{K}$ , a longitudinal temperature of 1 mK, an average velocity of order 1 m/s, and an atom flux of about  $3 \times 10^7 \text{ s}^{-1}$ . Using a radio-frequency (RF) current of a fixed frequency  $\nu$  coupled directly into the guide wires, atoms exceeding a transverse energy of  $h\nu$  have been continuously and selectively removed from the atomic beam. We have further constructed a Zeeman slower that is intended to enable high-flux operation of the atom guide. High atom flux will be essential in achieving cw evaporative atomic-beam cooling, cw BEC and cw atom lasing. In the following, the work is reviewed in detail.

#### A. Magnetic atom guide

Atoms in low-magnetic-field-seeking states are attracted to the minimum of the magnetic-dipole potential  $V(\mathbf{r}) = m_F g_F \mu_B |B(\mathbf{r})|$ . Here,  $^{87}\text{Rb}$  atoms in the state  $|F = 1, m_F = -1\rangle$  are used, which has a g-factor  $g_F = -1/2$ . The atoms are guided in a two-dimensional (transverse) quadrupole field, which is created using the two-wire geometry shown in Fig. 1. As indicated by the classical atomic trajectory in Fig. 1, low-field-seeking atoms are confined close to a propagation axis ( $z$ -axis), which is coincident with the symmetry line between the wires. To achieve strong magnetic compression, high transverse oscillation frequencies and high elastic collision rates, it is desirable to maximize the gradient of the  $B$ -field produced by the wire pair,  $\frac{\partial B}{\partial \rho} = \frac{4\mu_0 I}{\pi b^2}$ . There,  $b$  is the center-to-center wire separation and  $I$  the current.

The magnetic atom guide fabricated in this project has about 1.8 m length and uses in-vacuum hollow wires with an outer diameter of 3.175 mm and a center-to-center separation  $b$  as low as 4.175 mm. The guide is precision-mounted in the vacuum on a steel rail using alumina and aluminum spacers as well as Kapton foil. The mounts are designed such that a well-defined wire separation  $b$  is maintained, while the guide wires can still slide in longitudinal direction. Since differential thermal expansion of up to  $\sim 1$  mm occurs along the 2 m long wire segments, the latter aspect is crucial in the overall design. The wires are cooled using a closed, high-pressure water circuit. At  $I = 300$  A, the magnetic-field gradient reaches values of 2700 Gauss/cm, generating accelerations of 90 g on  $^{87}\text{Rb}$  atoms in the state  $|F = 1, m_F = -1\rangle$ . The system is routinely operated using the continuous-mode parameters listed in Table 1.

The cooling water is circulated by a heat exchanger with a high-pressure pump. Fault conditions in water pressure, flow, or temperature are detected and cause automatic shutdown. Among a couple of experiments with similar goals, the described guide has the largest transverse field gradient, allowing one to reach the best magnetic-compression

REPORT DOCUMENTATION PAGE			Form Approved OMB NO. 0704-0188	
Public Reporting burden for this collection of information is estimated to average 1 hour per response, including the time for reviewing instructions, searching existing data sources, gathering and maintaining the data needed, and completing and reviewing the collection of information. Send comment regarding this burden estimates or any other aspect of this collection of information, including suggestions for reducing this burden, to Washington Headquarters Services, Directorate for information Operations and Reports, 1215 Jefferson Davis Highway, Suite 1204, Arlington, VA 22202-4302, and to the Office of Management and Budget, Paperwork Reduction Project (0704-0188,) Washington, DC 20503.				
1. AGENCY USE ONLY (Leave Blank)		2. REPORT DATE 08/04/2006		3. REPORT TYPE AND DATES COVERED Final Progress Report, 7/1/2002- 4/30/2006
4. TITLE AND SUBTITLE CW Atom Laser			5. FUNDING NUMBERS DAAD 19-02-1-0273	
6. AUTHOR(S) G. Raithel				
7. PERFORMING ORGANIZATION NAME(S) AND ADDRESS(ES) University of Michigan, 450 Church St., Ann Arbor, MI 48109			8. PERFORMING ORGANIZATION REPORT NUMBER	
9. SPONSORING / MONITORING AGENCY NAME(S) AND ADDRESS(ES) U. S. Army Research Office P.O. Box 12211 Research Triangle Park, NC 27709-2211			10. SPONSORING / MONITORING AGENCY REPORT NUMBER 42791.3-PH	
11. SUPPLEMENTARY NOTES The views, opinions and/or findings contained in this report are those of the author(s) and should not be construed as an official Department of the Army position, policy or decision, unless so designated by other documentation.				
12 a. DISTRIBUTION / AVAILABILITY STATEMENT Approved for public release; distribution unlimited.			12 b. DISTRIBUTION CODE	
13. ABSTRACT (Maximum 200 words)  A continuous-wave (cw), phase- and amplitude-stable atom laser based on magnetic guiding, magnetic compression, and continuous distributed evaporative cooling has been pursued. The continuous operation of a cold atomic beam in a high-gradient (up to 2.7kG/cm) magnetic guide of 1.7m length has been demonstrated. An imaging method has been developed that allows in-situ measurements of atom temperatures and fluxes. The atomic beam in the high-gradient portion of the guide has been found to have a transverse temperature of 420 micro-Kelvin, a longitudinal temperature of 1mK, an average velocity of order 1m/s, and a flux of about 3x10 <sup>7</sup> per second. Using a radio-frequency current coupled directly into the guide wires, relatively hot atoms have been continuously and selectively removed from the atomic beam. A Zeeman slower has been constructed that will enable atom fluxes exceeding 10 <sup>9</sup> per second, as required for efficient evaporative atomic-beam cooling. In the project, the foundations have been laid to prepare a cw Bose-Einstein condensate and a coherent cw matter-wave beam in the guide. This matter-wave source will be ideal for atom-interferometric field- and motion sensors, which may become important in future sensing and navigation applications.				
14. SUBJECT TERMS CW Atom Laser			15. NUMBER OF PAGES 11	
			16. PRICE CODE	
17. SECURITY CLASSIFICATION OR REPORT UNCLASSIFIED	18. SECURITY CLASSIFICATION ON THIS PAGE UNCLASSIFIED	19. SECURITY CLASSIFICATION OF ABSTRACT UNCLASSIFIED	20. LIMITATION OF ABSTRACT UL	

NSN 7540-01-280-5500

Standard Form 298 (Rev.2-89)  
Prescribed by ANSI Std. Z39-18  
298-102

Enclosure 1

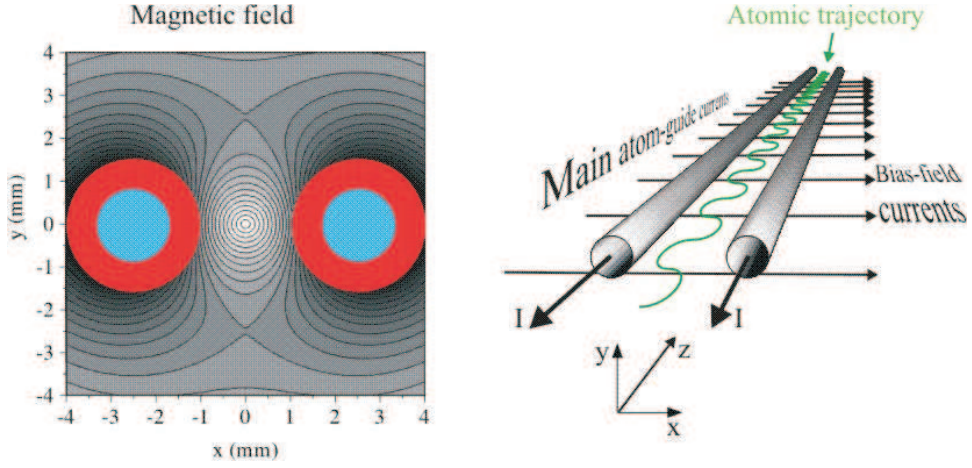


FIG. 1: Magnetic field (left panel) of basic atomic waveguide and classical trajectory of a guided atom (right panel). The magnetic guiding field is a 2D-quadrupole field generated by two parallel currents. In the left panel, the water-cooled wires have a center-to-center separation of 5 mm and a current of 300 A (red), and the field contour lines are separated by 20 Gauss. The transverse currents in right panel create a small bias magnetic field in  $z$ -direction.

Guide current	300 A
Field gradient (end of guide)	2.7 kGauss/cm
Dissipated power	3.2 kW
Cooling water pressure	120 PSI
Water inlet temperature	16°C
Water temperature differential	30°C
Vacuum pressure (horizontal guide region)	$8 \times 10^{-11}$ Torr

TABLE I: Parameters of continuous-mode operation of the magnetic atom guide.

factors. This aspect is important for effective evaporative cooling. Also, large transverse gradient implies a large transverse oscillation frequency of the atoms, simplifying the use of the guide in experiments that require single-transverse-mode atom guiding.

## B. Atomic-flow injection

The primary atomic beam is generated by a vapor-pressure pyramidal magneto-optical trap (PMOT; [1]), which is a modified version of a standard magneto-optical trap (MOT [2]). The utilized pyramidal MOT emits a cold atomic beam through a hole in the apex of the pyramid, similar to a Low-Velocity Intense Source of atoms (LVIS [3]). A high-power laser (power  $\sim 100$  mW measured at the PMOT) and 2" optics is used to operate the PMOT. The atomic beam emitted from the pyramidal MOT has been investigated in a set of absorption measurements. The flux is of order  $3 \times 10^9 \text{ s}^{-1}$ , the angular spread of order 50 mrad, the average velocity of  $\approx 22$  m/s, and the longitudinal velocity spread 16 m/s (FWHM).

The atomic beam emitted by the PMOT propagates into the differentially pumped UHV section of the setup that contains the atom guide. As shown in Fig. 2, the guide is comprised of a vertical injection/launch section of about 0.3 m height and a horizontal evaporative cooling section of 1.5 m length. A side-loading scheme is used in which the horizontal atomic beam emitted by the PMOT intersects with the vertical injection/launch section of the atom guide at a right angle. The injection is accomplished using a so-called "moving MOT".

In the "moving MOT", four laser beams forming a 2D-MOT are directed at the intersection point of the horizontal primary atomic beam and the vertical launch section of the guide. In that region, the guide wires provide a 2D quadrupole field with a field gradient of about 25 Gauss/cm. As Fig. 2 shows, the four 2D-MOT beams consist of a pair with upward and a pair with downward directions. The beams with downward direction are operated at a slightly lower frequency than the ones with upward direction. All beams are red-detuned from the  $^{87}\text{Rb } 5S_{1/2} \text{ F}=2 \rightarrow ^{87}\text{Rb } 5P_{3/2} \text{ F}=3$  transition; the average detuning is of order two line-widths (*i.e.*, about 12 MHz). The beams are circularly

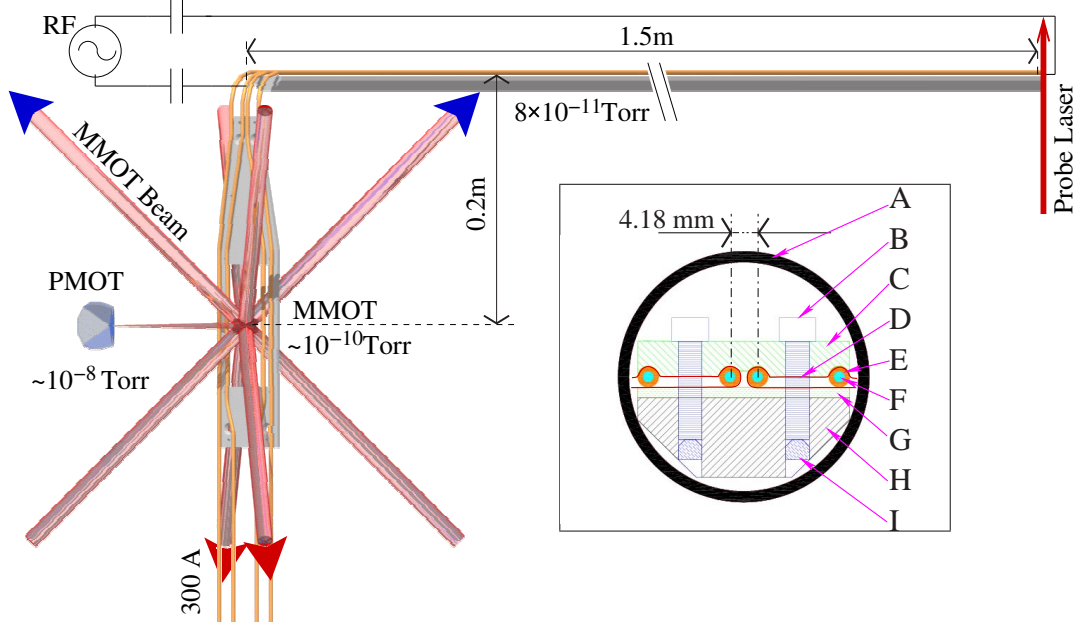


FIG. 2: Sketch of the experimental setup. Atoms are injected from a pyramidal magneto-optical trap (PMOT) via a "Moving MOT" (MMOT) into the vertical injection/launch section of a magnetic atom guide. As the injected atomic flow rises upward, it slows under the influence of gravity and becomes magnetically compressed. The flow then propagates into a long horizontal guide section. A radio-frequency current coupled into the horizontal guide section is used to remove the most energetic atoms from the guided atomic flow. The system has three differentially pumped vacuum regions, the pressure values of which are shown. The inset on the right shows a cross section through the horizontal section of the guide. (A) Vacuum chamber, (B) mounting screws, (C) aluminum spacers, (D) insulating Kapton film, (E) guide wires, (F) coolant, (G) alumina spacers, (H) guide rail, (I) lock screws.

polarized in a suitable manner. This configuration of magnetic fields and laser beams results in a 2D "moving MOT" (MMOT) that compresses the spread-out atoms of the incident atomic beam into a small-diameter cylindrical region around the guide axis. The average velocity (= launch velocity) of the atoms is exactly parallel to the atom-guide axis, which in the launch section is oriented vertical (see Fig. 2). The launch velocity can be tuned by varying the frequency difference of the up-going and down-going MMOT beams. In the frame of reference of the moving atoms, the frequencies of the four MMOT beams are doppler-shifted such that all beams have the same frequency. Using absorption measurements, it was found that the MMOT emits about  $5 \times 10^8$  atoms per second. Thus, the transfer efficiency from the PMOT beam into the MMOT is slightly below 20%.

Each atom emerging from the MMOT *must* traverse through the fringe fields of the four MMOT laser beams. Accurate control of the beam shapes and intensities of the four MMOT beams in the fringe-field regions is virtually impossible. Therefore, any extracted atom would experience strong, random differential radiation pressures in the fringe fields of the MMOT beams, causing the velocity to change in an erratic manner. The solution to this problem is dark-state extraction, *i. e.* optical pumping of the atoms into a "dark state" that does not scatter any MMOT photons. The optical pumping into the dark state needs to occur inside the MMOT volume, *before* the atoms reach the fringe fields of the MMOT laser beams. As explained in Ref. [4], the location of the optical pumping into the dark state is defined through a staggered arrangement of a MMOT re-pumper beam with a sharp upper knife-edge and a de-pumper beam with a sharp lower knife-edge. Any overlap between the re-pumper and the de-pumper beams needs to be avoided, while a gap up to 1 mm width is allowable. The knife-edge planes are oriented orthogonal to the direction of the extracted atomic beam (which propagates vertically in Fig. 2). The MMOT re-pumper beam is, as usual, resonant with the  $^{87}\text{Rb } 5S_{1/2} F=2 \rightarrow ^{87}\text{Rb } 5P_{3/2} F=3$  transition, while the de-pumper is resonant with the  $^{87}\text{Rb } 5S_{1/2} F=2 \rightarrow ^{87}\text{Rb } 5P_{3/2} F=2$  transition. This arrangement causes a transfer of the atoms into the dark state  $F=1$  at a location between the well-defined knife-edges of the re-pumper and the de-pumper beams. Statistically, one-third of the dark-state atoms will exit the MMOT in the magnetically guided sublevel  $m_F = -1$  (about  $2 \times 10^8$  in the present case).

As seen in Fig. 2, the atoms are launched vertically into the guide. There have been a couple of motivations for the vertical-launch design. One is that the MMOT only operates well at significant extraction velocities ( $\geq 2$  m/s). While the MMOT can be tuned to lower extraction velocities, the performance at lower velocities drops due to increasing susceptibility to spurious differential radiation pressure effects and to an increasing susceptibility of the

extracted magnetically guided dark-state atoms to off-resonant optical pumping. Therefore, it is necessary to run the MMOT at an extraction velocity of a few m/s. Since such velocities are not compatible with the formation of an in-line stationary BEC in the guide, gravitational slowing in the vertical guide section is used to remove most of the non-thermal, directed kinetic energy. Using the vertical launch system, the atoms are slowed down by gravity in the approximately 20 cm high vertical launch section of the guide. The atoms then traverse a 90-degree bend that directs the atomic flow onto the main 1.5 m long horizontal evaporative-cooling section of the guide. Another motivation for having a vertical launch section and a horizontal evaporative-cooling section has been that most of the stray light from the MMOT region is trapped in the 90-degree bend connecting the two sections.

### C. Magnetic compression

The atom guide is tapered [5, 6], *i.e.* the distance between the inner pair of guide tubes decreases from about 3.7 cm at the location where cold atoms are transferred from the MMOT into the guide down to 5.17 mm in the 90-degree bend. The field gradient increases from about 20 Gauss/cm at the MMOT to 1.7 kGauss/cm in the 90-degree bend. Through the 90-degree bend, the wire separation (and thus the  $B$ -gradient) remain fixed. Along the 1.5m long horizontal guide section the wire separation is further reduced, causing a further gradual increase of the gradient to 2700 Gauss/cm. A crucial benefit of the gradient increase is that the atomic distribution becomes magnetically compressed in the transverse directions as the atoms propagate through the tapered region. The compression enhances the collision rate and will thus facilitate evaporative cooling. Under typical conditions, the atomic flux is reduced by a factor of order two due to partial reflection of the atomic flow in the tapered section of the guide [5, 6]. The reflection occurs due to an adiabatic conservation of the action of the transverse motion,  $S_{\perp} = \oint \mathbf{p}_{\perp} \cdot d\mathbf{q}_{\perp}$ . The reflected atoms are not lost altogether, because they fall back into the MMOT and become recycled. Further, with a sufficient collision rate the gas flow will tend to become hydrodynamic, and a smaller fraction of atoms will become reflected.

### D. Analysis of the guided atomic beam

The analysis of the guided beam is performed in continuous-mode atomic-beam operation, with the guide field always on. To minimize probe-light scattering on the shiny guide tubes and to achieve well-defined beam intensities in the detection volume, the re-pumper and probe laser beams are merged into a common single-mode fiber. The fiber output is collimated and directed onto an aperture of <1 mm diameter, such that the intensity variation of the beam profile immediately behind the aperture plane is negligible. Using a long-focal-length lens, the aperture is imaged into the detection volume, creating a circular probe region of about 1 mm in diameter with a top-hat intensity profile. The fluorescence of the atoms in that probe region is then observed using a scientific CCD camera. To obtain undistorted images of the atomic flow, the flow is probed in a strobed mode (*i.e.* continuous atomic beam, but pulsed detection). The light pulses are typically 20  $\mu$ s long and therefore short enough that the atoms do not significantly move during the illumination period. The separation between the pulses typically is 1 ms, which is long enough that at each probe pulse the previously probed atomic-beam segment has cleared the detection volume, and an unperturbed new segment has filled the detection volume. By accumulating many strobed probe measurements, undistorted images of the atomic beam can be obtained.

The best method to measure atom distributions and temperatures in the guide is to only use re-pumper light in the probe region, with an intensity of order of the saturation intensity of the cycling transition (1.6 mW/cm<sup>2</sup>). The duration of the strobe intervals (20  $\mu$ s) is sufficiently long that all atoms inside the detection volume scatter of order two re-pumper photons and become optically pumped into the  $F = 2$  state. Notably, this even applies to the atoms traveling in the wings of the atomic flow, which experience large Zeeman shifts. Each atom in the probe volume therefore produces the same amount of fluorescence signal during detection, independent of the magnetic field at which the atom is located. Due to this uniformity of the signal obtained per atom, images obtained with only re-pumper light are proportional to the atomic-flow density projected onto the image plane. This property of repumper-only images allows for a reliable, quantitative in-situ analysis of the magnetically guided atomic beam. A slight disadvantage of repumper-only images is that the total photon yield per atom is only of order two, *i.e.* the images are quite dim.

Using the described method, the atomic flow has been analyzed immediately before the 90-degree bend and at the end of the guide. Typical images, beam-profiles and deduced temperatures are provided in Fig. 3. Using time-of-flight measurements, typical longitudinal temperatures and average forward velocities of the atoms in the horizontal guide section have been found to be 1 mK and 1.2 m/s.

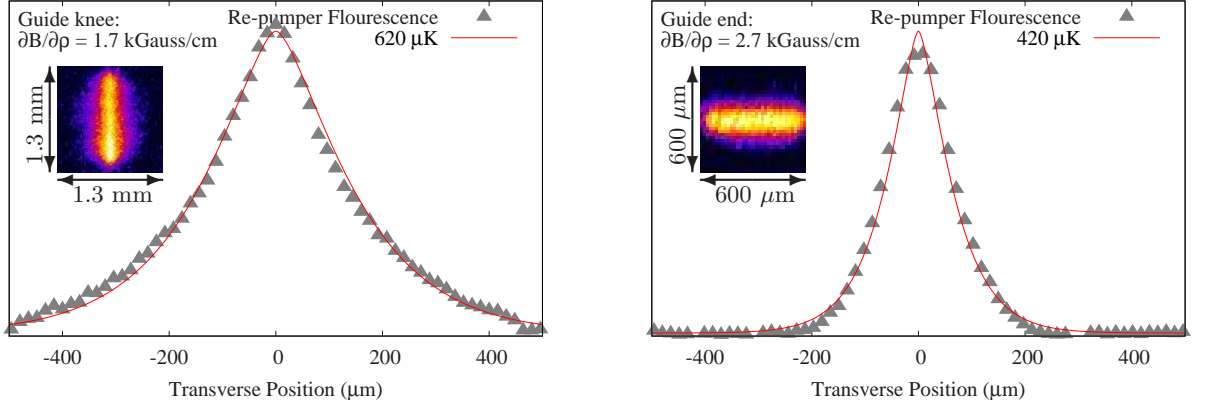


FIG. 3: **Left:** Atomic-beam image (inset) and corresponding profile transverse to the guide axis (data points). The image is obtained at a location just below the atom-guide knee with re-pumping light only. In the image, the guide axis is vertical. The line through the data points represents a fit for a temperature of 620  $\mu\text{K}$ . **Right:** Atomic-beam image obtained at the end of the atom guide with re-pumping light only (inset), and corresponding profile transverse to the guide axis (data points). In the image, the guide axis is horizontal. The line through the data points represents a fit for a temperature of 420  $\mu\text{K}$ .

Quantitative measurements of the atomic flow rates (flux) are of particular interest, because the atom flux has to exceed a critical value of order  $10^9 \text{ s}^{-1}$  for evaporative cooling to become effective. Using atomic-beam images obtained with the re-pumper only, a measurement of the atom flux in the guide has been performed. The method relies on the fact that the total photon yield per atom for re-pumper light is quite well known (about two photons per atom). Important parameters entering into the calculation are the geometric collection efficiency of the camera lens, as well as the pixel yield of the camera per photon reaching the CCD chip. An analysis along these lines for a launch velocity of 2.5 m/s has yielded an atomic flux of  $3 \times 10^7 \text{ s}^{-1}$  and a central volume density of about  $1 \times 10^9 \text{ cm}^{-3}$  at the end of the guide, with uncertainties less than a factor of two. The s-wave elastic collision rate (cross section  $\sigma = 700 \text{ nm}^2$ ) at this density and at a temperature of 500  $\mu\text{K}$  is about 0.5 per second, corresponding to of order one elastic collision of any given atom during its passage through the atom guide.

### E. Continuous RF-induced energy-selective removal of atoms

Precursor to realizing forced evaporative cooling, an RF-current is coupled onto one of the guide tubes in the horizontal guide section (see Fig. 2). Since the RF is directly coupled onto the guide tube, most of the RF-induced magnetic field is confined to the region between the tubes. The RF magnetic field is transverse to the guide axis and has a component transverse to the local static magnetic field practically everywhere on the evaporation surface. The benefits of this RF-coupling scheme include low RF-power requirements as well as low RF interference.

Fig. 4 shows profiles of the atomic beam at the end of the guide for continuously applied RF-currents at a frequency of 9 MHz and the indicated values of the estimated RF magnetic field. At 9 MHz RF frequency, a large portion of the atomic beam is above the evaporation threshold  $2\pi\hbar \times 9 \text{ MHz}$  (= the “RF knife-edge”) and should become removed if the RF-coupling scheme is effective. Fig. 4 shows that an applied RF  $B$ -field of a few 100 mG is sufficient for continuous RF-induced removal of practically all atoms above the “RF knife-edge”. In the figure, we also compare the measured fluorescence profiles with a fit for a thermal distribution function ( $T_{\perp} = 500 \mu\text{K}$ , red curve in Fig. 4) and the same distribution truncated at an energy of  $2\pi\hbar \times 9 \text{ MHz}$ . There is reasonably good agreement between the calculated curves and the respective measured profiles with no RF and 0.46 Gauss RF-field.

It is noted that the experimental curves are wider than the calculated ones by  $\sim 20 \mu\text{m}$ . The experimental broadening is due to diffraction effects and image smearing associated with the camera pixel size. Integrating the experimental data in Fig. 4, it is found that 16% of the atoms are left after energy-selective removal of atoms exceeding a transverse energy of  $2\pi\hbar \times 9 \text{ MHz}$ . Using a calculation, the average potential energy of the atoms remaining after the RF-induced atom removal is found to equal  $\approx 11 \%$  of the average potential energy without RF-induced atom removal.



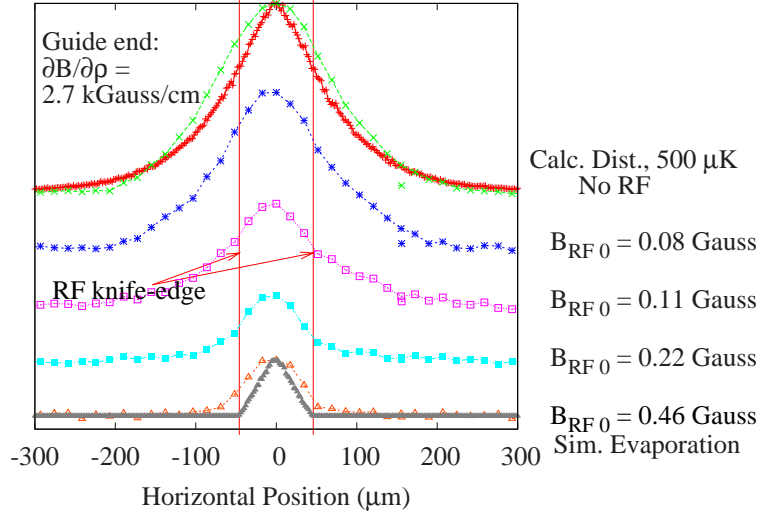


FIG. 4: Atomic-beam profiles transverse to the guide axis at the end of the atom guide, obtained with re-pumping light only and with a continuous radio-frequency (RF) current of 9 MHz frequency. The RF current is coupled onto a guide tube in the horizontal guide section. Estimates of the RF magnetic fields are provided. RF-induced removal of atoms outside the indicated “RF knife-edges” is clearly visible. The RF-induced atom removal saturates at about  $B_{\text{RF}} = 500$  mGauss. The experimental data agree reasonably well with calculations for a thermal distribution with  $T_{\perp} = 500$   $\mu\text{K}$  (red curve) and the same thermal distribution truncated at the “RF knife-edge” (gray curve). Both theoretical curves are scaled with the same factor to match the experimental data.

## F. Theory

A suite of tools has been developed to simulate important processes of the atom laser. Two major categories of interest are the optical cooling in the MMOT and the continuous evaporative cooling in the high-gradient portion of the magnetic atom guide.

As a part of this effort, in collaboration with Prof. Andrew Christlieb from the UM Math department a collisional modeling code has been developed and employed primarily for the purpose of simulating the pre-condensation evaporative process of the atom laser. This code involves a novel gridless implementation of Direct Simulation Monté Carlo (DSMC) [7]. As a particle method first developed to find solutions for the Boltzmann equation in rarefied gas flows (where continuous methods fail and computational resources required for direct solution of the Boltzmann equation are prohibitive), DSMC has been used successfully in a wide range of collisional systems. DSMC mandates the notion of nearest-neighbor groupings for the purpose of appropriately simulating the collision process of a system of particles. Typical DSMC involves mapping particles onto a fixed (or slowly evolving) grid, where collisions only occur between particles in the same grid cell. This mapping is intimately bound to the geometry of the physical system and mismatch can result in an erroneous solution. Furthermore, a change in the physical system often requires major changes in the code.

The novelty of the developed code stems from the use of a hierarchical tree algorithm to provide for localization of nearest neighbors. A major advantage of sorting with this approach comes from the fact that the geometry of the physical system is removed from the details of the code. This allows one to easily test arbitrary magnetic field geometries without the need to revamp or change the DSMC code. An additional advantage is faster convergence that occurs because statistical noise in the simulation is spread over the entire system rather than lumping together and moving through different simulated spatial locations. This enables one to determine the quality of a given evaporation plan more quickly. Similar tree algorithms have been very successful in calculations for long-range force problems [8] such as in gravitational [9] or plasma systems [10]. A simulation result of the initial dynamics of atoms in a magnetic guide is shown in Fig. 5.

The implementation of a continuous-wave atom laser design and exploration of its parameter space are non-trivial. While the components in the present apparatus have been designed to be modular, large changes on a day-to-day basis remain difficult. Thus, the various components present in the system define the range of parameter space that can be explored for a length of time on the order of weeks to months. As stated, the purpose of the simulation suite is to aid in the determination of good system parameters, such that the time-table for attaining a continuous-wave atom laser is significantly reduced. Already the DSMC code has been helpful in determining (or ruling out) possible

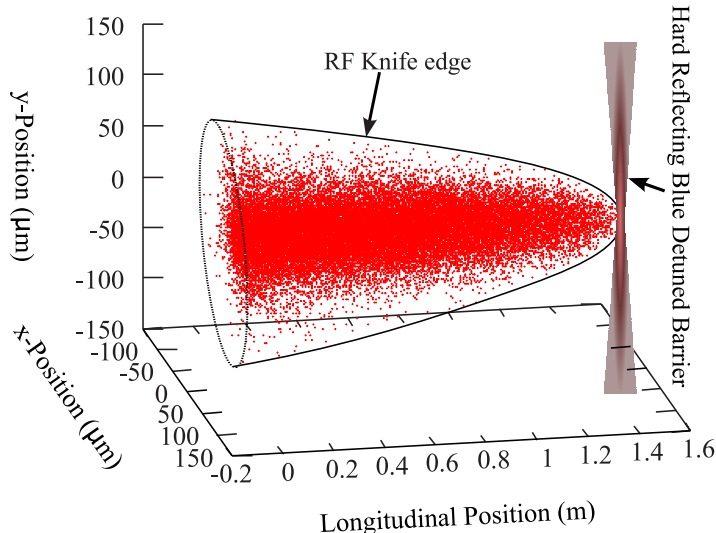


FIG. 5: Simulation of collisions in the atom guide with a linearly dropping RF-induced evaporation edge. The figure shows the atom distribution in the start-up phase of evaporative atomic-beam cooling.

evaporation schemes. Additionally, codes to simulate the optical cooling section of the apparatus have revealed a promising method to improve the MMOT such that initial collision rates and phase-space densities could be increased by about an order of magnitude.

### G. Increase of the injection rate

Of order 500 collisions per atom will be needed to cool the atomic flow to quantum degeneracy [11, 12]. A reasonable estimate based on presently achieved conditions is that the injection rate of atoms into the guide needs to be increased by a factor of a few 100, corresponding to initial on-axis densities of a few  $10^{11} \text{ cm}^{-3}$ , collision rates of a few  $100 \text{ s}^{-1}$ , and collision lengths of a few mm. While slight modifications in operating conditions will probably allow one to increase the flux by a factor of ten, at least another order of magnitude will be required. In order to increase the injected atomic flux by several orders of magnitude, a Zeeman slower has been built that will replace the PMOT. The utilized rubidium oven follows a design in Ref. [13], which is optimized such that it produces an effusive Maxwell velocity distribution rather than a supersonic distribution (the latter would not work well with a Zeeman slower). An outline of the Rb oven and Zeeman slower unit is provided in Fig. 6.

The Zeeman slower has been tested and performs as expected, as shown in Fig. 7. Without any transverse beam cooling, it already provides a flux of about 30 times as much as the PMOT flux (see Sec. IIB). Using the Zeeman slower as a primary atomic beam source, the magnetically guided atomic beam will become sufficiently dense so that efficient evaporative cooling can occur.

## III. PUBLICATIONS

### (a) Papers published in peer-reviewed journals

“Continuous propagation and energy filtering of a cold atomic beam in a long high-gradient magnetic atom guide,” Spencer E. Olson, Rahul R. Mhaskar, and Georg Raithel, *Phys. Rev. A* **73**, 033622 (2006).

### (b) Papers in conference proceedings

“Manipulation of magnetically guided atomic beams,” DAMOP 2004, *Bulletin of the APS* **49/3**, 13 (2004).

“Continuous propagation of magnetically guided dark-state  $^{87}\text{Rb}$ ,” DAMOP 2005, *Bulletin of the APS* **50/3**, 120 (2005).

“Open-channel fluorescence imaging of atoms in a high-gradient magnetic guide,” DAMOP 2006, *Bulletin of the APS* **51/3**, 61 (2005).

### (d) Manuscripts submitted

“Open-channel fluorescence imaging of atoms in high-gradient magnetic fields,” Rahul R. Mhaskar, Spencer E. Olson and Georg Raithel (2006).



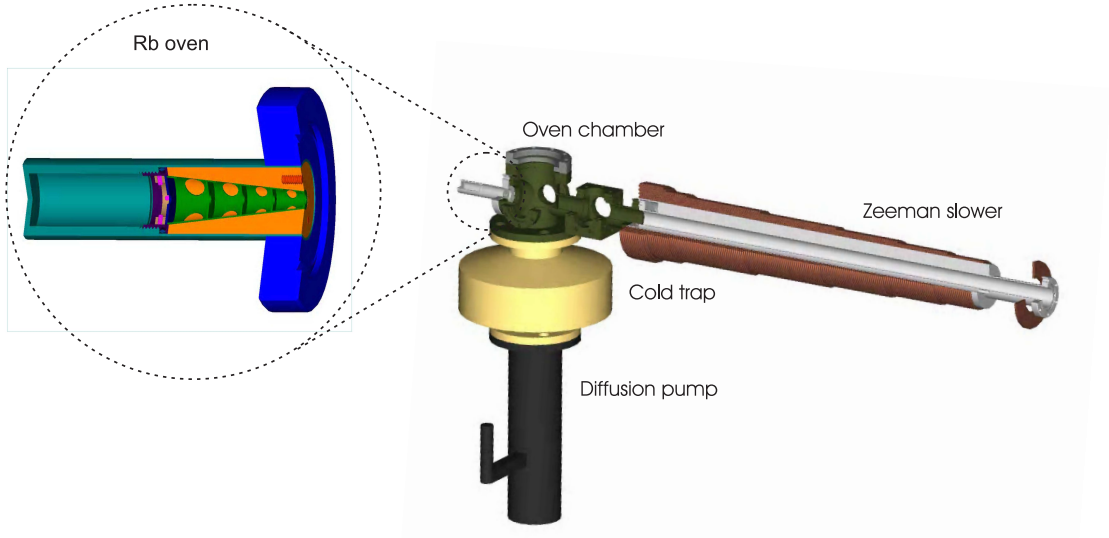


FIG. 6: Outline drawing of the Zeeman slower. The coil package of the slower contains a large section and a small extraction coil with opposite current directions. The large section is wound on a water-cooled jacket that surrounds the vacuum tube and cools the coil package from the inside. The vacuum chamber includes view-ports before and after the slower for transverse laser cooling, atomic-beam deflection, and beam analysis. The detail on the left shows a cutout view of the atomic-beam oven.

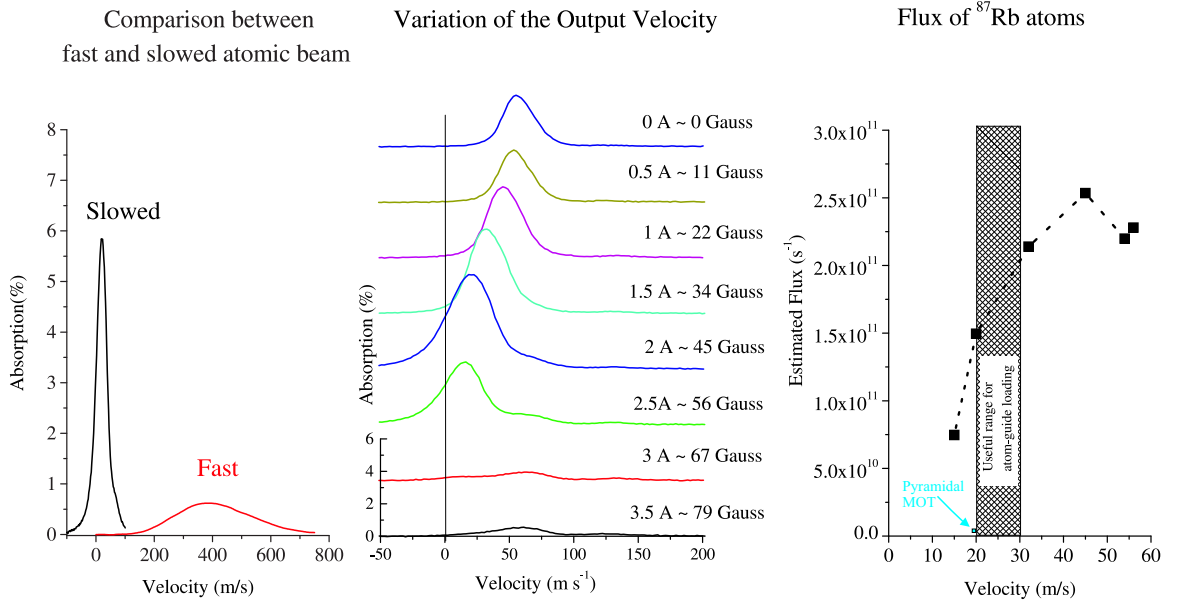


FIG. 7: Zeeman slower performance. Left: Comparison between typical velocity distributions of thermal (red) and slowed (black) atomic beams. Center: Velocity distributions of slowed atomic beams for the indicated values of the extraction magnetic field. Right: Beam flux vs extraction velocity for Zeeman slower (black) and PMOT source (blue).

#### IV. SCIENTIFIC PERSONNEL

G. Raithel, PI.

S. Olson, graduate student, graduated in May 2006. He currently is employed as a NRC post-doc at the NRL in Washington, DC.

R. Mhaskar, graduate student.

R. van de Wesep, undergraduate student.

E. Harding, undergraduate student.

## V. BIBLIOGRAPHY

---

- [1] K. I. Lee, J. A. Kim, H. R. Noh, and W. Jhe, *Opt. Lett.* **21**, 1177 (1996).
- [2] E. L. Raab, M. G. Prentiss, A. E. Cable, A. Clairon, S. Chu, and D. E. Pritchard, *Phys. Rev. Lett.* **59**, 2631 (1987).
- [3] Z. T. Lu, K. L. Corwin, M. J. Renn, M. H. Anderson, E. A. Cornell, and C. E. Wieman, *Phys. Rev. Lett.* **77**, 3331 (1996).
- [4] B. Teo, T. Cubel, and G. Raithel, *Opt. Commun.* **212**, 307 (2002).
- [5] B. Teo and G. Raithel, *Phys. Rev. A* **63**, 031402 (2001).
- [6] B. Teo and G. Raithel, *Phys. Rev. A* **65**, 51401 (2002).
- [7] G. A. Bird, *Molecular Gas Dynamics and the Direct Simulation of Gas Flows* (Oxford University Press, 1994).
- [8] J. Barnes and P. Hut, *Nature* **324**, 446 (1986).
- [9] V. Springel, N. Yoshida, and S. D. M. White, *New Astronomy* **6**, 79 (2001).
- [10] A. J. Christlieb, R. Krasny, and J. P. Verboncoeur, *Comp. Phys. Comm.* **164**, 306 (2004).
- [11] E. Mandonnet, A. Minguzzi, R. Dum, I. Carusotto, Y. Castin, and J. Dalibard, *Eur. Phys. J. D* **10**, 9 (2000).
- [12] Y. Castin, R. Dum, E. Mandonnet, A. Minguzzi, and I. Carusotto, *Journal of Modern Optics* **47**, 2671 (2000).
- [13] R. D. Swenunson and U. Even, *Rev. Sci. Instr.* **52**, 559 (1981).